Eur Biophys J (2012) 41:425–436
DOI 10.1007/s00249-012-0795-7

ORIGINAL PAPER

EBSA
Biophysics in Europe

Unusual salt-induced behaviour of guanine-rich natural DNA evidenced by dynamic light scattering

Massimo Zimbone · Gabriele Bonaventura · Pietro Baeri · Maria Luisa Barcellona

Received: 4 August 2011 / Revised: 5 January 2012 / Accepted: 13 January 2012 / Published online: 19 February 2012

Abstract The appearance of the slow mode, revealed by dynamic light scattering (DLS) measurements in *Micrococcus luteus* DNA with high GC content, and the effect of guanine sequences on changes of DNA physical state and conformational transitions were investigated. We used two different spectroscopic approaches: DLS, to evidence the relatively slowly diffusing particles arising at high salt concentration, ascribable to the formation of large unspecific molecular aggregates, and circular dichroism spectroscopy, to identify these entities. Our results bring us to conclude that a peculiar, unconventional, structural transition, due to the presence of long guanine stretches, in a well-defined experimental condition, can occur. We comment on the biological implications to detect, by spectroscopic measurements, such an unusual structure involved in the stability, protection and replication maintenance along the human telomeric G-rich strand.

Keywords DLS · Self-assembly · G-quadruplexes · Structural transition · DNA

Introduction

DNA in aqueous solution exhibits self-aggregation phenomena that, in the last few years, have been usefully evidenced by dynamic light scattering (DLS).

M. Zimbone (✉) · P. Baeri
Dipartimento di Fisica e Astronomia, Università di Catania, 6, Viale A. Doria, 95125 Catania, Italy
e-mail: massimo.zimbone@ct.infn.it

G. Bonaventura · M. L. Barcellona
Dipartimento di Scienze del Farmaco, Sezione di Biochimica, Università di Catania, 6, Viale A. Doria, 95125 Catania, Italy

DLS experiments are a valuable approach for the observation of differently collapsed states of condensed, aggregated or compacted DNA molecules. The time autocorrelation function of the scattered light intensity is the common method used in DLS experiments to describe its intensity fluctuation. It is generally analysed in terms of a series of decay time constants or frequency distribution, each of them being attributed to a particular particle motion (Provencher and Stepanek 1996).

During the last 2 decades, the behaviour of DNA and of other polyelectrolytes in buffered solution has been extensively investigated by DLS. A peculiar feature, often evidenced in the scattered light autocorrelation function, is the presence of an unexpected very large decay time. This so-called "slow mode" is observed in the frequency distribution of the inverse Laplace's transform of the autocorrelation function. It appears as a broad peak around a mean value that is about one order of magnitude lower than the frequency correlated with the translation motions of a single DNA chain. The frequency distribution, in these conditions, becomes bimodal (and sometimes even trimodal since a peak associated with some fast internal or rotational motion of the single chain can be evidenced, too) (Sorlie and Pecora 1988).

The slow mode has been associated with a sort of translational Brownian motion of objects moving with an extremely low diffusion coefficient. It has been observed in a variety of oligodeoxynucleotides, both linear fragments and circular covalently closed (Sorlie and Pecora 1988; Goinga and Pecora 1999; Ferrari and Bloomfield 1992; Newman et al. 1994; Seils and Pecora 1995; Borsali et al. 1998), with chain length ranging from about 20 base pairs up to about 2,000. Moreover, it has been observed both in the case where the DNA chain is well described by a rigid rod and in the case of a short chain linear DNA, (160 bp

long) (Goinga and Pecora 1999) or small duplex oligonucleotides, (20 bp long), (Borsali et al. 1998) and in the case where it is better described by a coil (Ferrari and Bloomfield 1992; Newman et al. 1994; Seils and Pecora 1995).

For longer DNA chains, no measurements obtained by DLS are reported. However, a recent observation of Brownian motion of entangled linear and circular DNA molecules up to 45 kbp long has evidenced a reduction of the translational diffusion coefficient that, in specific salt concentration and DNA conditions, may become even three orders of magnitude lower than the one of the single molecule (Skibinska et al. 1999). This reduction has been correlated with the formation of large domains of entangled DNA chains, and the decreased mobility has been attributed both to slow motion of the entire domain itself and to the reduced mobility of the single molecule inside the domain.

As a matter of fact, the origin of this slow mode remains uncertain, although the more common explanation seems to be correlated with large polydispersed multi-chain aggregates, which are formed in conditions of high polymer concentration and/or low ionic strength. SAXS analysis on 20-bp oligonucleotides evidenced an X-ray peak correlated to the slow mode, indicating the presence of local order in the solution (Borsali et al. 1998). This fact strongly supports the association of the slow mode with the formation of some kind of aggregates not related to a simple, incomplete dissolution of DNA but, instead, to some kind of structured self-assembly.

There is, moreover, a high specificity of the non-covalent interactions between particular DNA sequences, i.e. guanine sequences, that can lead to a different suitability in determining self-assembly DNA process.

Explanations different from the casual formation of disordered multi-chain aggregates have been developed (Goinga and Pecora 1999, Robertson and Smith 2007); they have been linked to some sequence specificity occurring in DNA molecules. For example, the formation of stable multistranded DNA complexes, thermally activated, made by long terminal tracks of guanines, called frayed wires, has been reported (Sedlak 1996; Protozanova and Macgregor 2000). In this case, the appearance of the slow mode is no longer determined by salt or DNA concentration alone, but is determined by the relative amount of guanine bases among the different numbers of strands, the constituent of the population of high-order aggregates, differing in sizes and molecular weights (Poon and Macgregor 2000; Borovok et al. 2008). The biomolecular self-assembly of DNA bases, particularly guanine bases (G) and their derivatives, have attracted considerable interest in recent years, in consideration of their uniqueness to form quadruplex structures known to be stabilised by Hoogsteen hydrogen bonding between four guanines and to influence genomic stability (Kunstelj et al. 2007; Patel et al. 2007; Phan et al. 2006; Simonsson 2001). It is ascertained that G-quadruplex secondary structures deviate from canonical B-form double-stranded DNA (Williamson 1994), and, since it is present in G-rich regions of the human genome, representing the human telomeric DNA, comprising thousands of tandem repeats of a G-rich sequence (micro satellites or mini satellites) (Simonsson 2001), its study has received emphasis and growing attention (Burge et al. 2006; Maiti 2010; Lipps and Rhodes 2009).

G-4 DNA structures inducing processes, such as condensation and denaturation, may occur in vivo, and there is evidence suggesting that such an event happens, under physiological temperature, ph and ionic conditions, (i.e. Na^+ and K^+ salt stabilised), also in vitro (Huppert 2008; Maizels 2006; Qin and Hurley 2007). Despite such evidence the functional role of G-4 nucleic acid in living cells is still controversial, although a considerable number of potential quadruplex sequences are present at the 5′-end of human genes, but not in the coding region (Brooks et al. 2007; Lim et al. 2009).

In this work, we give evidence of a case of slow mode appearance in a DNA aqueous solution that seems to be related to some specificity of the DNA primary sequence. We place our attention on the peculiar behaviour of *Micrococcus luteus* DNA, which is known to have a G + C (guanine–cytosine) base content in the order of 72%, and we compared it to the behaviour of more common DNAs having an almost equal percentage of A + T and G + C base content.

Experimental procedure

Materials, characterisation and sample preparation

We expressed the molecular weight of DNA by its length, in base pair, bp, constituents of the entire molecule. Each base pair is 0.34 nm long and has an average molecular weight of 660 Dalton.

The following samples were used (all of them were lyophilized ultra pure):

1. Calf thymus DNA ≈20-kbp DNA fragments purchased from Sigma-Aldrich, Molecular Biology Division.
2. *Micrococcus luteus* ≈2,000-bp DNA fragments (kindly gived by Dr. S. Stefani, Department of Microbiology, University of Catania).
3. Herring sperm ≈3,000-bp DNA fragments purchased by Sigma-Aldrich, Molecular Biology Division.
4. Poly d(G–C) ≈1,000-bp fragments purchased from Sigma Aldrich, Molecular Biology Division.

5. Poly d(A–T) ≈700-bp fragments, purchased from Sigma Aldrich, Molecular Biology Division.

All of them were lyophilized starting from a solution containing 1 mM Tris-HCl (pH 7.5) with 1 mM NaCl and 1 mM EDTA, then stored at 4°C.

Inorganic chemicals were of the highest purity available, and doubly distilled water was used. All samples are linear double-stranded DNA.

To maintain this configuration the polymers were rehydrated with 10 mM Tris-HCl buffer solution, pH 7.5, containing 1 mM EDTA and NaCl at a concentration ranging from 10 mM to 2 M. EDTA was added in order to chelate any amount of multiple charged ions and to prevent nucleases from DNA degradation.

The buffer was passed through 100-nm pore Millex GP filters immediately prior to DNA dissolution.

All natural DNA samples were checked for the average polymer length by agarose gel electrophoresis, (1% w/v), in Tris/acetate (TAE) buffer, in the presence of 0.5 μg/ml ethidium bromide, except for calf thymus DNA, (0.5% agarose gel). For the alternating copolymers poly d(GC) and poly d(AT), an approximate average length in base pairs of 1,000 and 700, respectively, was evaluated by the same procedure.

DNA concentration was then adjusted by UV absorption at a maximum absorption wavelength of 260 nm to a value between 50 and 75 μg/ml. The concentration of the polymer solutions was determined by using the following molar extinction coefficients at 254 nm for *M. luteus* DNA (8,400 M^{-1} cm^{-1}), at 262 nm for calf thymus and herring sperm DNA, (6,600 M^{-1} cm^{-1}), at 254 nm for the poly d(GC) (8,400 M^{-1} cm^{-1}) and at 262 nm for the poly d(AT) (6,600 M^{-1} cm^{-1}).

The absorption ratio at 260 and 280 nm was calculated in order to provide an estimation of the polynucleotide purity and integrity: A_{260}/A_{280} was 1.9.

Care was taken in order to achieve complete solubility of DNA by gentle stirring at 4°C, overnight. No filtering was adopted after dissolution in order to leave aggregates, if any, well detectable. However, the samples were centrifuged at 5,000 rpm to remove air bubbles and possible dust.

After the introduction into pre-cleaned scattering cells, samples were allowed to equilibrate at room temperature (20–22°C) for a few hours before acquiring light-scattering measurements.

At least four samples for each DNA type in the presence of different NaCl concentrations were prepared and analysed on different days in order to assure result reproducibility and a satisfying evaluation of the significant statistical error.

Light scattering equipment and data analysis

Light scattering measurements were performed by a homemade apparatus using a quartz scattering cell, confocal collecting optics, a Hamamatzu photomultiplier mounted on a rotating arm, a BI-9100 AT hardware logarithmic correlator (Brookhaven Instruments Corp.) and illuminating the sample with a 30 mW, 632 nm, He–Ne laser. Appropriate diaphragms and spherical lens were adopted in order to have the smallest possible coherence area in the nearest region to the focus. The scattering angle was held fixed at 90°.

DLS measurements provided the evaluation of the auto-correlation function.

$$Y(t) = \lim_{T\to\infty} \left(\int_0^T I(\tau) \cdot I(\tau + t) \mathrm{d}\tau \right) \Big/ T$$

of the scattered light intensity, I, with light-beating technique in homodyne mode.

After evaluation of the baseline B of $Y(t)$, the electric field correlation function g_1 can be evaluated via the Siegert relation:

$$g_1(t) = (Y(t)/B - 1)^{1/2}$$

The g_1 function decreases monotonically with time and for a homogeneous monodisperse solution of spherical particles is a single decreasing exponential:

$$g_1 = A \exp(-\Gamma t)$$

where the frequency Γ is directly connected with the translational diffusion coefficient D by the equation: $\Gamma = Dq^2$ where q is the scattering vector defined as:

$$q = (4\pi n/\lambda)\sin(\theta/2)$$

where n, λ and θ are the refraction index of the solvent, the light wavelength and the scattering angle, respectively.

Moreover, the hydrodynamic radius R_h, i.e. the radius of the sphere having a given diffusion coefficient D, is:

$$R_h = kT/6\pi\eta D$$

where k is the Boltzmann constant, T the temperature and η the liquid viscosity coefficient

Mixtures of differently sized particles show a field auto-correlation function, which is a sum of several exponential decay components, with different Γs related to particles having different frictions with the surrounding medium due either to their shape or size. Polymers or non-spherical objects may exhibit other exponential components in the auto-correlation function due to internal or rotational motions that, in general, are evidenced at values of Γ much higher than those connected with the translational motion

of the same objects. In the present article, we will neither show nor discuss these high Γ values components.

We have analysed the auto-correlation functions both by multiexponential fitting and CONTIN analysis (Provencher 1982; Zimbone et al. 2009). CONTIN analysis auto-correlation data used a constrained and conditioned inverse Laplace transform technique. It finds the smoothest non-negative distribution of decay times that is consistent with data, and it gives, as a result, the distribution of the decay frequencies, Γs, of the exponential functions that compose the entire electric field auto-correlation function.

In the following, in order to expose our results and to compare several samples between them, we will report the normalised auto-correlation function of the signal intensity, which is the measured auto-correlation function $Y(t)$ after base subtraction and normalised to the unity: $Y_{\text{norm}} = (Y(t) - B)/(Y(0) - B)$. We will also show the CONTIN distribution of the Γs for the same samples.

CD spectroscopy and melting temperature measurements

CD

Circular dichroism (CD) spectroscopy is a powerful method for studying DNA conformational properties and for rapidly evaluating the effect of changing environment on DNA behaviour and to follow structural transitions among DNA structural families.

CD measurements were performed with a Jasco J 715 A dichrograph, calibrated with Tris-EDTA buffer 10 mM, ph 7.5, at room temperature. A quartz cuvette with 1-mm path length was used for all the CD experiments. Spectra were recorded between 200- and 340-nm wavelengths. Each CD spectrum was an average of three scans.

As a baseline, the solvent reference spectrum was used and automatically subtracted from the CD spectrum of each sample.

CD band intensities were expressed as $\Delta\varepsilon$ (M^{-1} cm^{-1}).

Tm measurements

UV light absorption spectra of DNA molecules strongly depend on their degree of denaturation.

We performed a series of measurements to study the effect of temperature on the state of aggregation and salt concentration induced of *M. luteus* DNA and of poly d(G–C) to investigate the different contribution of the two polymer species given not only to the slow mode peak, but also to the occurrence of guanine stretch peculiar re-arrangements concerning the natural DNA. The thermal behaviour and the absorbance profiles for the two polymer samples, at a concentration of 50 μg/ml roughly corresponding to 1 OD, were analysed. Samples were dissolved in an aqueous buffer solution containing 10 mM Tris-HCl and 1 mM EDTA at pH 7.5. Each polymer spectrum, monitoring the melting profiles by UV absorption between 200 and 340 nm, was recorded in the presence of different sodium salt concentrations (i.e. 10 mM and 2 M NaCl) at increasing temperature in the interval between 25 and 95°C.

The spectra acquisition was carried out on a Cary 300 Bio UV-VIS double-beam spectrophotometer equipped with a single position Peltier temperature control system. The heating and cooling rates were 0.5°C per minute.

Experimental results

Light-scattering measurements

Figure 1 reports the normalised autocorrelation functions, Y_{norm}, obtained at 90° scattering angle for three double-strand natural DNAs in solution with 10 mM NaCl concentration (open dots) and 2 M NaCl concentration (full dots). In the case of herring sperm DNA (Fig. 1a) and calf thymus DNA (Fig. 1b), the autocorrelation functions for both salt concentrations are very similar. The decay time is about 1 and 0.4 ms for calf thymus and herring sperm DNAs, respectively, and is almost insensitive to the NaCl concentration variations. Instead, for *M. luteus* DNA (Fig. 1c), the autocorrelation function depends strongly on the salt concentration. In fact, the decay time is 0.25 and 2 ms for 10 mM and 2 M NaCl concentration, respectively.

Inverse Laplace transforms of the field autocorrelation functions (CONTIN analysis) are shown in Fig. 2 where the Γ's distributions obtained at 10 mM NaCl concentration (open dots) and at 2 M NaCl concentration (full dots) for herring sperm DNA (Fig. 2a), calf thymus DNA (Fig. 2b) and *M. luteus* DNA (Fig. 2c) are reported.

In all cases, two groups of Γ components dominate the distribution: the former between 1,000 and 2,000 s^{-1} and the latter at about 100–200 s^{-1}, indicating the presence of two families of objects having a diffusion coefficient of the order of 10^{-7} and 10^{-8} cm^2/s, respectively. The faster group can be associated to objects having a hydrodynamic radius of the order of 50–100 nm and it is easily assigned to the motion of solitary DNA molecules. The slower one is recognised as the "slow mode". It could be associated with larger objects having a hydrodynamic radius of the order of some μm. The exact position of the peak in the Γ's distribution associated to the single molecule translation is determined by the DNA chain length. It corresponds to an average hydrodynamic radius of 100, 60 and 40 nm for 20,000 bp calf thymus, 3,000 bp herring sperm and 2,000 bp *M. luteus* DNA, respectively. These values are

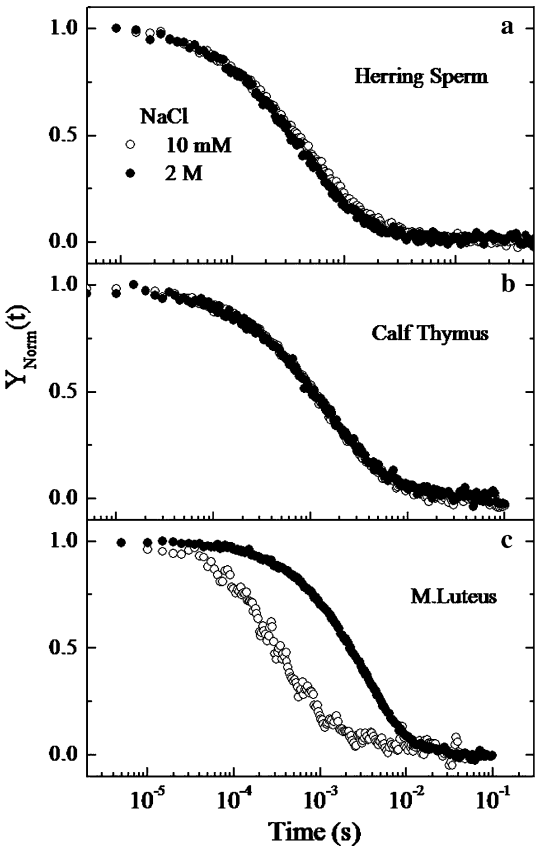

Fig. 1 Normalised autocorrelation functions for DLS analysis with 632-nm wavelength, 90° scattering angle of three natural double-stranded DNAs, 50 μg/ml, aqueous buffered solution with 10 mM NaCl concentration (*open dots*) or 1 M NaCl concentration (*full dots*). **a** 3,000 bp herring sperm DNA, **b** 20 kbp calf thymus, **c** 2,000 bp *M. luteus*

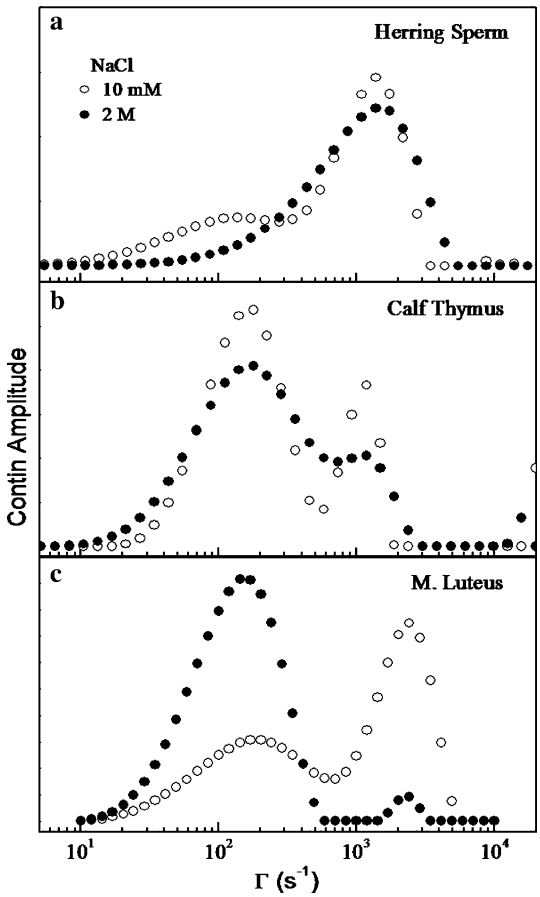

Fig. 2 Amplitude distribution of the Γ components as derived by CONTIN analysis of the six correlation function shown in Fig. 1

congruent with those reported in the literature for the length of such (Zimbone et al. 2009).

In the case of herring sperm DNA, the slow mode peak decreases with increasing the salt concentration and almost disappears at 2 M concentration. This result is in accordance to the other cases, already cited in the "Introduction". In the case of calf thymus DNA, the ratio between the slow and the fast mode peak is almost unchanged by going from 10 mM to 2 M NaCl concentration. *M. luteus* Γ's distributions, instead, are very different for the two salt concentrations employed. Although the smaller peak, related to the slow mode, for the 10 mM NaCl concentration sample, appears very similar in amplitude to the one observed for herring sperm DNA, in the sample at 2 M NaCl it is instead much larger. A satisfactory fit of the corresponding g_1 function was also obtained by a two exponential fit that gave, consistently with CONTIN analysis, two time decay constants of approximately 1 and 0.6 ms. The relative amplitude of the slow mode in the double exponential analysis is defined as the amplitude of the slowly decaying exponential divided by the sum of the fast and slow decay exponentials. In the CONTIN analysis, the relative amplitude is defined as the sum of the components under the slow mode peak divided by the sum of all the components, excluding the ones, if detected, related to the internal motion of DNA molecules, which appears as small peaks at very high Γ values (not shown here). The two methods of fitting gave very similar results within the experimental errors.

The relative amplitude of the slow mode peak for *M. luteus* DNA is reported in Fig. 3 as a function of the salt concentration. It is almost independent of the salt concentration below 500 mM. For larger salt concentration values, it abruptly increases up to values near one, since it almost dominates Γ's entire distribution, as seen in the full dotted distribution shown in Fig. 2c. Error bars in the figure represent the fluctuation of the results obtained in different measurements.

The slow-moving objects may be either the same DNA molecules that for some reason have lowered the diffusion coefficient or are aggregates of several molecules leading to a unique larger particle that suffers major friction during its translational motion. In this latter case, the mass of the scattering object is also increased, and this should affect

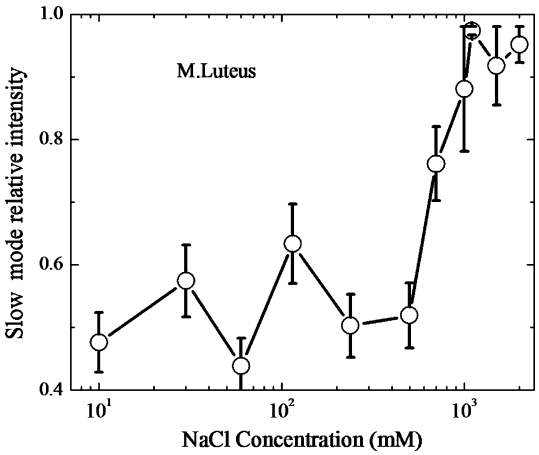

Fig. 3 Relative amplitude of the slow mode for 2,000 bp *M. luteus* DNA in buffered aqueous solution as a function of NaCl concentration

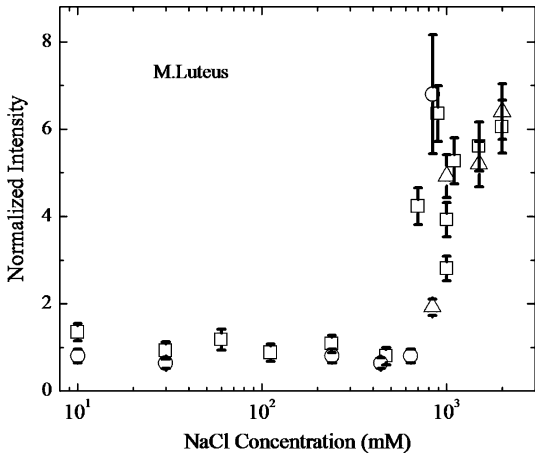

Fig. 4 Intensity of light scattered at 90° from an aqueous buffered solution of *M. luteus* DNA (2,000 bp) as a function of NaCl concentration. *Different symbols* refer to different sets of samples

the scattered light intensity, too. For this reason, we measured the absolute scattering intensity, obtained with the same laser intensity and the same collecting geometry and electronic setup, on samples having the same DNA mass concentration but different salt concentrations.

The signal variation of the scattered light measured for different preparations of *M. luteus* DNA at a fixed DNA concentration as a function of NaCl concentration is reported in Fig. 4. It clearly shows a strong and abrupt increase of scattered light intensity of about a factor of 6.5 when the NaCl concentration becomes greater than 700 mM. This increase cannot be simply associated with the (well-known) enhancement of the light scattering intensity observed for biological macromolecules in the presence of high salt concentration (>1 M), since the latter is progressive and slow without any sudden change in correspondence of a particular salt concentration. Therefore, we conclude that this evidence indicates an aggregation of DNA molecules in particles with greater mass.

Since massive particles scatter more light than smaller ones, the relative concentration number of the aggregates is smaller than the relative amplitude of the slow mode. Although it is difficult to extract the amount of large and small particles in the sample from the slow mode relative amplitude, its consistent increase clearly indicates the presence of a much larger number of particles exhibiting larger friction at high salt concentration compared with the low salt concentration solution.

Since it is known that the GC content of *M. luteus* DNA (72%) is much higher than that of the other two analysed DNA (about 50%) coming from different sources, in order to explain the observed different behaviour concerning the spectroscopic and thermal assays, we performed the same measurements on the alternating copolymer poly d(A–T) and poly d(G–C). We pursued the target to verify by utilising the homogeneity of the two synthetic polynucleotides, if the prevalent composition in GC bases, in the former case, could be responsible for the observed anomalous responses.

Figure 5 shows the autocorrelation functions obtained at 10 mM and 2 M sodium salt concentration for poly d(AT), (Fig. 5a) and for poly d(GC), (Fig. 5b) polymers, respectively.

In Fig. 5a, no appreciable difference is observed for the two saline concentrations employed, similarly to the results obtained for calf thymus and herring sperm DNA.

In the case of poly d(G–C) polymer, Fig. 5b, on the contrary, the autocorrelation function, in the presence of 2 M NaCl, shows an average decay time of 0.9 ms, which is about four times greater than the one observed in the presence of 10 mM NaCl.

Moreover, inverse Laplace transforms of the field autocorrelation functions (CONTIN analysis), reported in Fig. 6, showed for the poly d(G–C) sample, with 10 mM and 2 M NaCl, respectively, a double-peaked Γ distribution, as exhibited by *M. luteus* DNA. It also exhibits a similar behaviour to that observed for the *M. luteus* DNA related to the slow mode component: it abruptly increases when the amount of NaCl exceeds a given value (of about 200 mM in this case). The relative amplitude of the slow mode peak, as a function of the salt concentration, is reported in Fig. 7.

It is evident that in either case, *M. luteus* or poly d(GC), a structural transition from a regime of quasi non-interacting objects, with DNA coils independently moving, to a regime in which they strongly interact takes place when the salt concentration is increased above a certain threshold value. Such an interaction causes a collapse in the DNA backbone, causing the formation of larger structures, characterised by a sort of agglomerated fragment made by new, free-moving, large particles. This transition happens

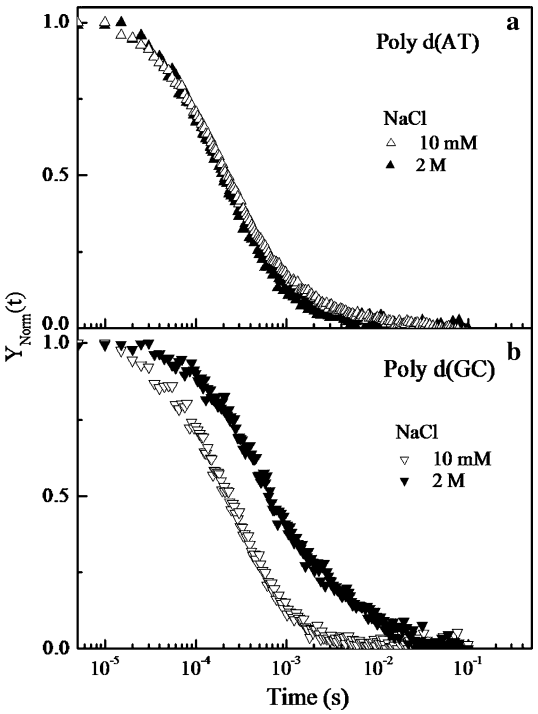

Fig. 5 Normalised autocorrelation functions for DLS analysis, with 632-nm wavelength at 90° scattering angle, of two alternating copolymers in aqueous buffered solution with 10 mM NaCl concentration (*open dots*) and with 2 M NaCl concentration (*full dots*). **a** Poly d(AT), **b** poly d(GC)

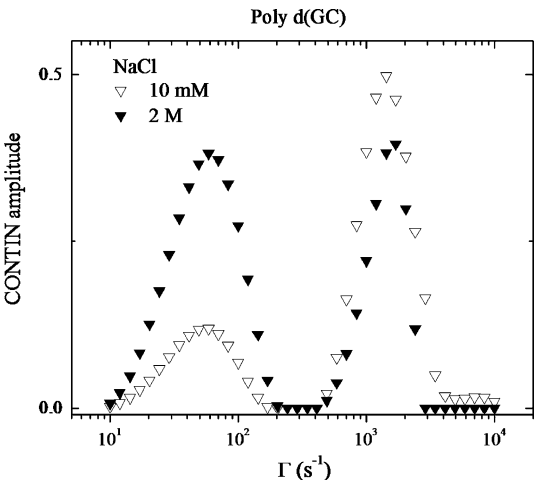

Fig. 6 Amplitude distribution of the Γ components as derived by CONTIN analysis of the two correlation functions shown in Fig. 5b

quite sharply at a given sodium salt concentration, which is positioned around 200 mM for the poly d(GC) polymer and around 700 mM for the *M. luteus* DNA; on the contrary it is not seen for the poly d(AT) sample nor for the other natural DNA assayed, having a lower GC content than that of the *M. luteus*.

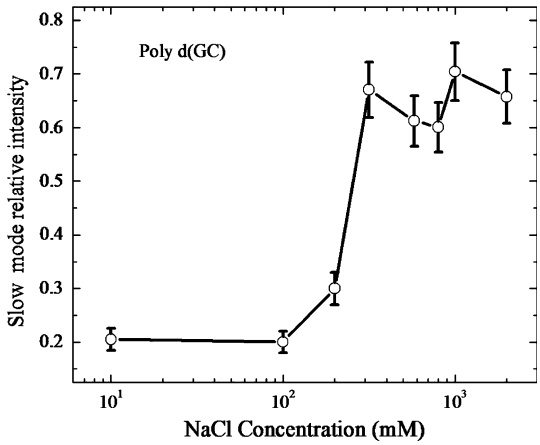

Fig. 7 Relative amplitude of the slow mode component for 50 μg/ml buffered solution of poly d(G–C) as a function of the NaCl concentration

Optical microscopy

Optical microscopy was also employed in order to characterise the *M. luteus* DNA samples. Figure 8 shows two dark fields, 100× magnification, for the sample with 10 mM (left side) and 2 M NaCl (right side), respectively. Images were obtained focussing the objective inside a liquid drop of DNA solution. In the 2 M NaCl sample, several bright spots are clearly visible, indicating the presence of particles at least as large as a fraction of the light wavelength, i.e. a minimum of several hundred nanometers. Instead, very few of these spots, are visible in the left side of the picture, i.e. in the presence of 10 mM NaCl.

CD spectroscopy (a) and melting temperature measurements (b)

(a) CD spectra of *M. luteus* DNA, as a prototype of natural DNA, and of poly d(GC) as synthetic polydeoxynucleotide, at two different NaCl concentrations, 10 mM and 2 M, respectively, were recorded. The CD spectra of native DNA from *M. luteus* (72% G + C), obtained in the presence of 10 mM (upper part) and 2 M (lower part) NaCl concentration, respectively, are shown in Fig. 9. The CD spectrum in the presence of 10 mM NaCl is characterised by a positive, broad band between 260 and 280 nm and by a negative band around 245 nm, referring to the B-DNA form where the base pairs are perpendicular to the double helix axis, conferring only a weak chirality. The spectrum, obtained for the solution containing 2 M NaCl, instead, exhibits a dominant positive band at 270 nm and an unexpected additional peak at 210 nm, most probably due to different stacking interaction with respect to the former CD spectrum recorded at low ionic strength.

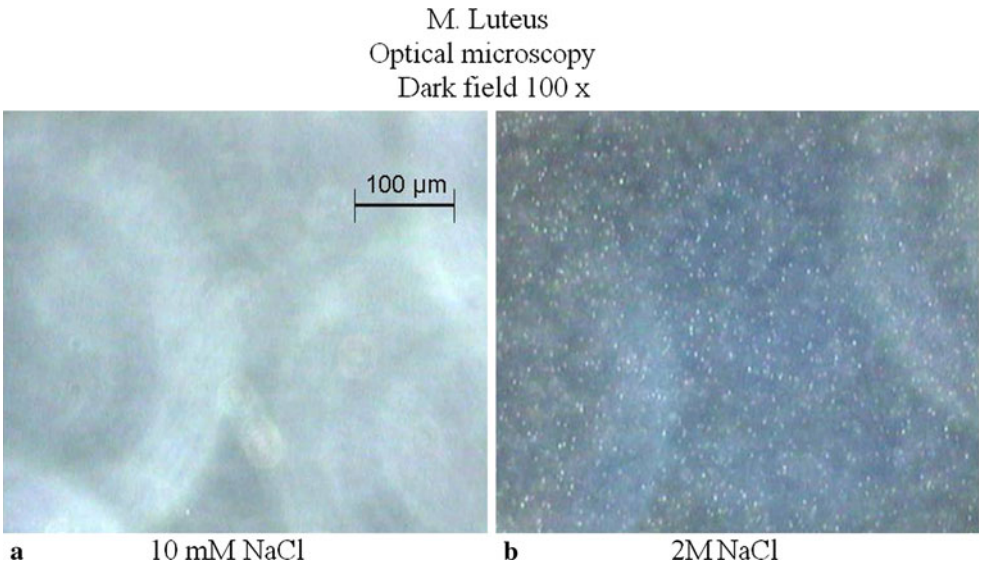

Fig. 8 Dark field optical microscopy images of *M. luteus* DNA in buffered water solution with 10 mM NaCl concentration (*left*) and 2 M NaCl concentration (*right*)

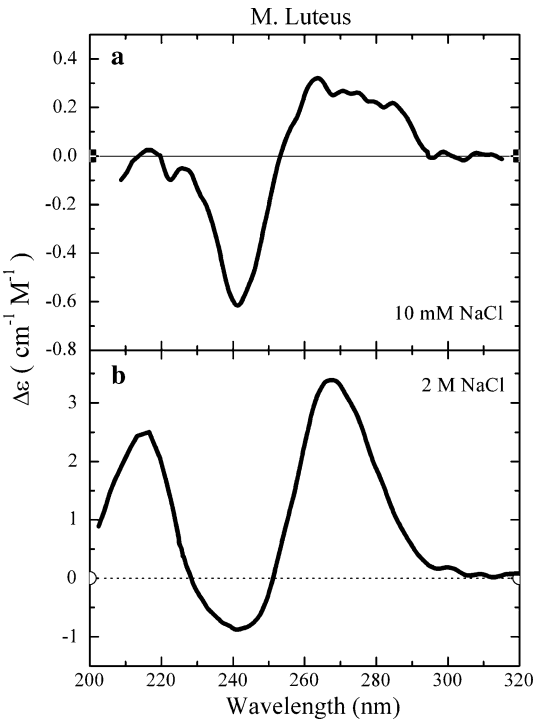

Fig. 9 CD spectra of *M. luteus* DNA in 2 M NaCl (*lower part*) and 10 mM (*upper part*) buffered water solution at room temperature

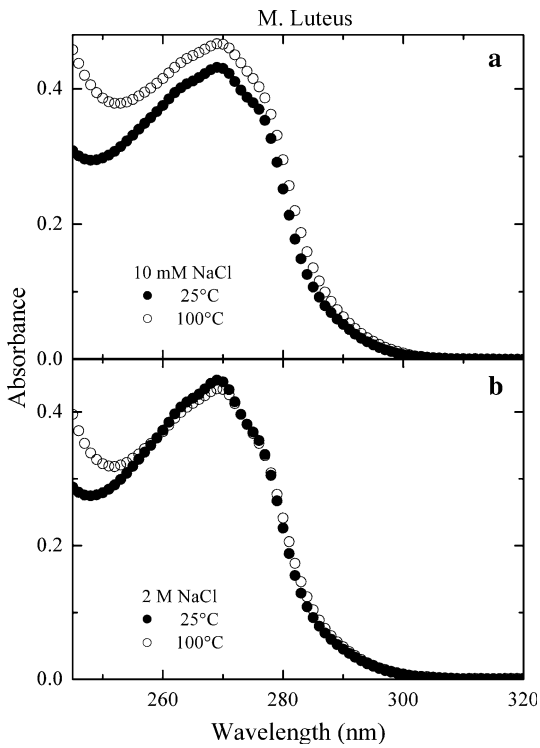

Fig. 10 UV absorption spectra of *M. luteus* DNA dissolved in TE buffer added by 10 mM NaCl (**a**) and 2 M NaCl (**b**) at a temperature of 25°C (*full dots*) and 100°C (*open dots*)

The CD spectrum of the alternating copolymer poly d(GC) and of the alternating copolymer poly d(AT), either in 10 mM or in 2 M NaCl, did not show any appreciable differences compared with the common, canonical features of a B-DNA family CD spectra (data not shown).

(b) In Fig. 10 we report the UV absorption spectra of *M. luteus* DNA recorded in the presence of different sodium salt concentrations [i.e. 10 mM (a) and 2 M NaCl (b)] at temperatures of 25°C (dark symbols) and 100°C (open symbols).

The UV melting curves of DNA in the presence of 10 mM NaCl show a gradual absorbance increase with a maximum wavelength of 265 nm, starting from 25°C up to 100°C, due to the hyperchromicity effect, as is expected upon denaturation. With increasing NaCl content up to

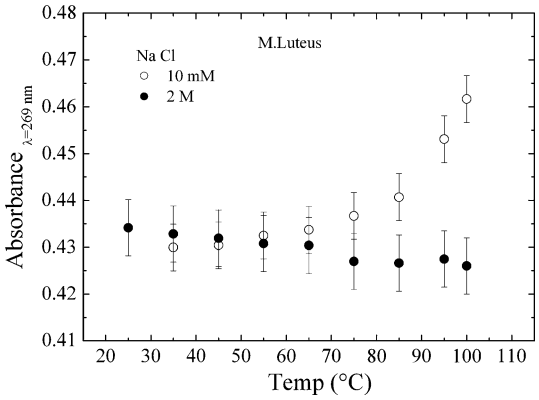

Fig. 11 Tm profiles (absorbance vs. temperature) of *M. luteus* DNA in 10 mM NaCl (*open dots*) and 2 M NaCl (*full dots*) recorded at the maximum absorption wavelength of 265 nm

2 M, a different UV profile is observed: due to the temperature variation, no detectable absorbance increase was shown. This result indicates that, for this DNA sample in our experimental conditions, the unusual tertiary structure of possibly occurring long guanine tracks, due to the high G–C content, is possible; it could adopt an intramolecular G-quadruplex structure, insensitive to the increasing melting temperature.

The different pattern obtained for the thermal curves of *M. luteus* DNA in 10 mM and 2 M NaCl, respectively, reported in Fig. 11, recorded at the maximum absorbance wavelength of 265 nm, visually stresses the suggestion that the unusual G-structures were already present at high salt concentration before heating.

Discussion and conclusion

According to previous literature reports, the intensity of the slow mode is sensitive to DNA concentration or to medium salt concentration in a reciprocal manner. In fact, for example, for short polymer chains (236 bp), the slow mode appeared for sodium salt concentrations below 10 mM and for DNA concentrations between 1 and 10 mg/ml. Instead, if the DNA concentration becomes higher, the slow mode was evidenced only if the salt concentration became about 100 mM (Goinga and Pecora 1999). In the case of longer DNA (2,311 bp plasmid Ferrari and Bloomfield 1992; Newman et al. 1994) the occurrence of the slow mode component has been evidenced for DNA concentrations higher than 0.15 mg/ml if the NaCl concentration was 1 mM, but if it was 150 mM, then the DNA concentration would have to be higher than 1 mg/ml.

Other experimental evidence, obtained by direct observation of Brownian motion, have shown, at low sodium salt concentration, one order of magnitude reduction in the translational diffusion coefficient at a DNA concentration of 1 mg/ml for 6-kbp long chains and at a DNA concentration of 0.3 mg/ml for 45-kbp long chains, respectively (Skibinska et al. 1999).

As a general rule it appears that the "slow mode" component should be negligible at a concentration of DNA below approximately 0.1 mg/ml and for salt concentration higher than 100 mM.

It has been also suggested (Goinga and Pecora 1999) that the slow mode becomes evident when the DNA concentration is above the so called "dilute regime", occurring when the average distance between molecules becomes comparable with the average size of the molecules themselves. If the chain length is below the persistence length, (about 50 nm), DNA molecules can be regarded as rigid and rod-like under a wide range of solution conditions. Therefore, the size of the molecules is assumed to be the contour length; for longer chains, instead, the adoption of the gyration diameter parameter seems more appropriate than the contour length.

The wormlike polymer model is commonly adopted to describe DNA fragments of some thousand base pair length (Zimbone et al. 2009). Following this model, in all our cases, the gyration radius is in the range between 50 nm (*M. luteus*) and 150 nm (calf thymus). The DNA concentration of 50 μg/ml adopted here is below the limit of a dilute solution, except in the case of calf thymus, whose average distance between DNA molecules is only a factor of two greater than the gyration diameter.

The data related to calf thymus, herring sperm and poly d(A–T) presented here are within this picture. In all cases, at 10 mM NaCl concentration, the slow mode amplitude is lower than the normal or "fast mode" amplitude. Moreover, as is well established by literature reports, its amplitude decreases or vanishes by increasing sodium salt concentration. This is clearly evident, at least in the case of medium base pair length fragments [e.g. 3,000 bp for herring sperm DNA and ~1,000 bp for poly d(AT)], by observing the CONTIN distribution reported in Fig. 2a and the tail of the correlation function in Figs. 1a and 5a. In the case of calf thymus DNA (20,000 bp), it is still appreciable also at high salt concentrations, even if, in this case, the DNA concentration is nearly close to the limit of dilute solution because of its large gyration radius.

In any case, the slow mode amplitude decreases, or at least it does not increase, by increasing the salt concentration.

A dramatically different behaviour for *M. luteus* DNA is observed. Its slow mode component, already present at 10 mM NaCl concentration, increases abruptly in the range between 500 and 1,000 mM NaCl concentration. The scattered light intensity variation for the same sample exhibited the same pattern (see Fig. 4) as a function of the

increasing salt concentration by supporting the idea that the slow mode is associated with the formation of more massive particles.

Optical microscope observations confirmed the presence of large-sized (from a few hundred nm up to a few microns) particles only in those samples where the salt concentration was high, whilst they were scarcely visible at low salt concentrations. This fact gives further confidence to the interpretation of the slow mode increase being due to the formation of large massive particles resulting from the aggregation of several DNA molecules, as already suggested by the increases of the scattering light intensity reported in Fig. 4. Without this light microscopy evidence, the slow mode could be interpreted in different ways. For example, it could be associated with the translation of slowed down single molecules inside some sort of dominium of entangled molecules interacting each other or to the movement of the entire dominium, which, however, cannot be interpreted as a single massive particle. Such an interpretation could be rather satisfactory for long DNA chains (Skibinska et al. 1999), and perhaps it is valid, in our case, for the 20,000-bp calf thymus DNA.

Since the scattered light intensity from particles of a given size depends on both their mass and their concentration, it is impossible to uniquely evaluate, from the data reported in Fig. 4, the number of molecules aggregated in a larger particle and the number of aggregates contributing to the slow mode from the present data. A rough estimation could result in six molecules in each aggregate if one assumes that all molecules were aggregated. Instead, if one assumes that, for example, only 5% of the molecules were aggregated, the observed scattered light intensity is consistent with the number of 100 molecules in each aggregate. This evaluation, however, represents only a lower limit to the number of aggregate molecules since we are not here taking into account the effect of the form factor of the scattered light intensity. For large particles, in fact, the fraction light scattered at 90° may be considerably lower than the one for a single molecule. If this could be evaluated, the intensities reported in Fig. 4 could be corrected to much higher values and so also the evaluation of the number of aggregated molecules.

It would have to be premised that the adopted pH allows total dissociation of hydrogen ions from the DNA molecule that, therefore, behaves as a complete ionised polyelectrolyte. In this condition, in the presence of counterions, the self-repulsion of the DNA segments is neutralised by converting the intramolecular repulsion into an attractive interaction. These two mechanisms are not mutually exclusive. By increasing the NaCl concentration, the intramolecular electrostatic repulsion between the negatively charged phosphate groups considerably decreases, and also decreases intermolecular electrostatic repulsion between DNA fragments, by causing a reduction of the electrostatic forces affecting the coil dimensions; therefore, a structural transition, like 'a collapse' can happen in the DNA backbone.

Afterwards, in the condensed DNA state the interaction between DNA molecules and counterions at high concentration is repulsive. In fact, the condensation process reduces the free energy of the transition to compact form by minimising the unfavourable interaction of DNA with the inducing molecules.

The long range inter polyion correlation, leading to the slow mode, could originate from the repulsive forces; on the other hand, there are many speculations in the literature about a sort of efficient attractive force between polyions arising from fluctuations in the counterions position (Borsali et al. 1998). Interplay between these forces and their dependence on the added-salt concentration variation could influence the intensity or even the appearance of the agglomerated molecular fraction.

There are, moreover, various experimental observations supporting the relevance of the intrinsic symmetry owned by the oligodeoxynucleotides with alternating A and T or G and C bases, along the two directions of the DNA molecule, which are likely responsible for the different kinds of DNA self-assembly.

Again, there is a high specificity of the non-covalent interactions between particular DNA sequences that can lead to a different ability in determining a certain kind of DNA self-assembly. For long polymer fragments, the naturally occurring sequence heterogeneity mitigates the differences.

However, the high percentage of guanine and cytosine in the *M. luteus* DNA base composition (72%) can lead to repetitive G-rich stretches along its chain, and, as a consequence, the specific interaction between different portions of the same chain (and/or with the other molecules) induced by counterions may be responsible for the observed anomalous behaviour.

The different results obtained with the poly d(GC) with respect to poly d(AT) polymers, increase the plausibility of this last statement.

The spectroscopic behaviour of the GC polymer is only qualitatively equal to that of *M. luteus* DNA. In fact, large and massive molecular aggregates are formed in both cases, but at a different salt concentration when a critical value is reached, which is 700 mM for *M. luteus* DNA and 200 mM for poly d(GC). In addition, the relative amplitude of the slow mode peak is different, being about 90% of the total signal intensity for *M. luteus* DNA and about 60% in the case of poly d(GC). As we expected, the poly d(AT) sample behaves like the other natural polydeoxynucleotides investigated. We ascribe the different observed salt concentrations at which such a transition happens

(700–200 mM) and also the different results obtained by CD and Tm measurements to an intrinsic different molecular base sequence, i.e. natural occurrence of homo stretching of G, which likely occurs in the *M. luteus*, but it is not possible in poly d(G–C) because it is an alternating copolymer.

In our case, the intrinsic restriction of DLS spectroscopy does not allow us to discriminate between different states and the structural reorganisation of naturally occurring purine bases repeats, even if this structural morphology could be the origin of the slow mode peak. The CD spectroscopy, by coupling the possibility of appreciating the differences between substantial deviations from canonical B-form, (e.g. unstacking Hoogsteen stabilised bases) and physical state transitions can answer the question. The CD spectrum, provides information on the alterations in the local structure or in the overall geometry of DNA produced at high salt molarities by the decreased water activity, influencing the properties of the bulk water around the hydrated DNA. Moreover, primarily over other methods, it changes sensitively in dependence on the base composition. In fact, a linear relation exists between the specific rotation at 270 nm and the G + C content, as we observed.

It is possible to restrict any sequence-dependent property of a nucleotide chain as a linear function of the properties of a limited number of nucleotides of simple sequences (nearest neighbour theory). Then any perturbation of such an assessment may be ascribed either to alterations in the geometrical parameters of the helix or to an unconventional structure, allowed by specific purine sequences, such as guanines repeat sequences, forming G-4 structures. The observation by CD measurements of a 210-nm positive peak, indicative of a plausible guanine tetrad formation together with a dominant positive band at 270 nm, is related to such a perturbation.

We would like to stress the known behaviour of guanine-guanine interaction, leading to a rare association of DNA molecules into greater structures. In this context, a physiologically relevant example is the formation of alternate DNA structures, deviating from B-form double-stranded DNA, such as the G-quadruplex, widely distributed throughout the human genome.

We must underline the functional involvement of this novel structure in the conformational heterogeneity of human telomeric sequences, where G-quadruplexes occur naturally (Verma et al. 2009) and, consequently, the important role played by these structures in telomere stability. An additional value is represented by some evidence reported in the literature suggesting a relation between known defects of G-quadruplex nucleic acids and human genetic diseases (Phan et al. 2007; McEachern et al. 2000; Palm and de Lange 2008).

The two combined experimental approaches, (DLS and CD) take a look inside the self-assembly process, induced by high salt concentration, from a different perspective: a physical transition state and a structural, conformational change. The significant experimental differences observed among the polydeoxynucleotides of different base composition under investigation lie in the primary sequence variability, natural versus synthetic polymers, that imply a different possibility of finding suitable G-rich sequences, as happens in the *M. luteus* DNA.

Another significant aspect of the G-repeat tandem is the possibility of offering, through a simple physical state modification approach, such as the agglomeration induced by high ionic strength, a DNA formulation suitable for gene delivery in in vitro cell cultures where ionic strengthes up to 1 M are used. In fact gene therapy, i.e. the DNA delivery into target cells, could have a more extended application if there was the possibility to transfect, in a safe and bioactive manner, DNA molecules through non-viral vectors (Wu and Brosh 2010; Lansdorp 2009; von Figura et al. 2009; Brown et al. 2001; Ewert et al. 2004; Hayes et al. 2006).

A different application of this surprising G-guanines stretch is the construction of new nanoscale electronic devices for industrial or diagnostic purposes that could profit from the use of strongly interacting DNA base self-assembly.

References

Borovok N, Iram N, Zikich D, Ghabboun J, Livshits GI, Porath D, Kotlyar AB (2008) Assembling of G-strands into novel tetramolecular parallel G4-DNA nanostructures using avidin-biotin recognition. NAR 36:5050–5060

Borsali R, Nguyen H, Pecora R (1998) Small angle neutron scattering and dynamic light scattering from polyelectrolytes: DNA. Macromolecules 31:1548

Brooks TA, Kendrick S, Hurley L (2007) Making sense of G-quadruplex and i-motif functions in oncogene promoters. FEBS J 277:3459–3469

Brown MD, Schatzlein AG, Uchegbu IF (2001) Gene delivery with synthetic (non viral) carriers. Int J Pharm 229:1–21

Burge S, Parkinson GN, Hazel P, Todd AK, Neidle S (2006) Quadruplex DNA: sequence, topology and structure. NAR 34:5402

Ewert K, Slack NL, Ahmad A, Evans HM, Lin AJ, Samuel CE, Safinya CR (2004) Cationic lipid-DNA complexes for gene therapy: understanding the relationship between complex structure and gene delivery pathways at the molecular level. Curr Med Chem 11:133–149

Ferrari ME, Bloomfield VA (1992) Scattering and diffusion of mononucleosomal DNA: effects of counterion valence and salt, and DNA concentration. Macromolecules 25:5266

Goinga HT, Pecora R (1999) Dynamics of low molecular weight DNA fragments in dilute and semidilute solutions. Macromolecules 24:6128

Hayes ME, Drummond DC, Kirpotin DB, Zheng WW, Noble CO, Park JW, Marks JD, Benz CC, Hong K (2006) Genospheres: self-assembling nucleic acid-lipid nanoparticles suitable for targeted gene delivery. Gene Ther 13:646–651

Huppert JL (2008) Hunting G-quadruplexes. Biochimie 90:1140–1148

Kunstelj K, Federiconi F, Spindler L, Drevensek-Olenik I (2007) Self-organization of guanosine 5′-monophosphate on mica. Colloids Surf B Biointerfaces 59:120–127

Lansdorp PM (2009) Telomeres and disease. EMBO J 28:2532

Lim KW, Amrane S, Bouaziz S, Xu W, Mu Y, Patel DJ, Luu KN, Phan AT (2009) Structure of the human telomere in K+ solution: a stable basket-type G-quadruplex with only two G-tetrad layers. J Am Chem Soc 131:4301–4309

Lipps HJ, Rhodes D (2009) G-quadruplex structures: in vivo evidence and function. Trends Cell Biol 19:414–422

Maiti S (2010) Human telomeric G-quadruplex. FEBSJ 277:1097

Maizels N (2006) Dynamic roles for G4 DNA in the biology of eukaryotic cells. Nat Struct Mol Biol 13:1055–1059

McEachern MJ, Krauskopf A, Blackburn EH (2000) Telomeres and their control. Ann Rev Genet 34:331

Newman A, Tracy B, Pecora R (1994) Dynamic light scattering from monodisperse 2311 base pair circular DNA: ionic strength dependence. Macromolecules 27:6808

Palm W, de Lange T (2008) How shelterin protects mammalian telomeres. Ann Rev Genet 42:301

Patel DJ, Phan AT, Kuryavyi V (2007) Human telomere, oncogenic promoter and 5′-UTR G-quadruplexes: diverse higher order DNA and RNA targets for cancer therapeutics. NAR 35:7429–7455

Phan AT, Kuryavyi V, Patel DJ (2006) DNA architecture: from G to Z. Curr Opin Struct Biol 16:288–298

Phan AT, Kuryavyi V, Luu KN, Patel DJ (2007) Structure of two intramolecular G-quadruplexes formed by natural human telomere sequences in K+ solution. NAR 35:6517

Poon K, Macgregor RB Jr (2000) Biophys Chem 84(3):205–216

Protozanova E, Macgregor RB Jr (2000) Thermal activation of DNA frayed wire formation. Biophys Chem 84:137

Provencher SW (1982) Contin: a general purpose constrained regularization program for inverting noisy linear algebraic and integral equations. Comput Phys Commun 27:229

Provencher SW, Stepanek P (1996) Global analysis of dynamic light scattering autocorrelation functions. Part Part Syst Charact 13:291

Qin YL, Hurley H (2007) Structures, folding patterns, and functions of intramolecular DNA G-quadruplexes found in eukaryotic promoter regions. Biochimie 90:1149–1171

Robertson RM, Smith DE (2007) Small-angle neutron scattering and dynamic light scattering from a polyelectrolyte solution: DNA. Macromolecules 40:3373

Sedlak M (1996) The ionic strength dependence oft he structure and dynamics of polyelectrolyte solution as seen by light scattering: the slow mode dilemma. J Chem Phys 105:10123

Seils J, Pecora R (1995) Dynamics of a 2311 base pair superhelical DNA in dilute and semidilute solutions. Macromolecules 28:661

Simonsson T (2001) G-quadruplex DNA structures variations on a theme. Biol Chem 382:621–628

Skibinska L, Gapinski J, Liu H, Patkowski A, Fischer EW, Pecora R (1999) Effects of electrostatic interaction on the structure and dynamics of a model electrolyte. II Intermolecular correlation. J Chem Phys 110:1794

Sorlie S, Pecora R (1988) A dynamic light scattering study of a 2311 base pair DNA restriction fragment. Macromolecules 21:1437–1449

Verma A, Yadav VK, Basundra R, Kumar A, Chowdhury S (2009) Evidence of genome-wide G4 DNA-mediated gene expression in human cancer cells. NAR 37:4194–4204

von Figura G, Hartmann D, Song Z, Rudolph KL (2009) Role of telomere dysfunction in aging and its detection by biomarkers. J Mol Med 87:1165

Williamson JR (1994) Annu Rev Biophys Biomol Struct 23:703–730

Wu Y, Brosh RM (2010) G-quadruplex nucleic acids and human disease. FEBS J 277:3470

Zimbone M, Baeri P, Barcellona M, Volti GL, Bonaventura G, Viscuso O (2009) Light scattering study of natural DNAs over a wide range of molecular weights: evidence for compaction of the large molecules. Int J Biol Macromol 45:242